First Order Magnetic Transition in Doped $CeFe_2$ Alloys: Phase Coexistence and Metastability

S. B. Roy,[1,2] G. K. Perkins,[1] M. K. Chattopadhyay,[2] A. K. Nigam,[3] K. J. S. Sokhey,[2] P. Chaddah,[2] A. D. Caplin,[1] and L. F. Cohen[1]

[1]*Blackett Laboratory, Imperial College, London SW7 2BZ, United Kingdom*
[2]*Low Temperature Physics Laboratory, Centre for Advanced Technology, Indore 452013, India*
[3]*Tata Institute of Fundamental Research, Mumbai 400005, India*

(Received 9 December 2003; published 9 April 2004)

First order ferromagnetic (FM) to antiferromagnetic (AFM) phase transition in doped $CeFe_2$ alloys is studied with the micro-Hall probe technique. Clear visual evidence of magnetic phase coexistence on micrometer scales and the evolution of this phase coexistence as a function of temperature, magnetic field, and time across the first order FM-AFM transition is presented. Such phase coexistence and metastability arise as a natural consequence of an intrinsic disorder-influenced first order transition. The generality of these phenomena involving other classes of materials is discussed.

DOI: 10.1103/PhysRevLett.92.147203 PACS numbers: 75.30.Kz

The effect of quenched disorder on a first order phase transition (FOPT) has been a subject of considerable scientific interest since the late 1970s [1]. In condensed matter physics, several distinct examples are known: disordered-ferroelectric transitions [2], precursor effects in martensitic transitions [3], the vortex-matter phases of high temperature superconductors (HTS) [4], and electronic phase separation in manganites showing colossal magnetoresistance [5]. Of these the last two areas have drawn much attention in recent years, although without general recognition that there exists some common underlying physics. Detailed computational studies [6,7] confirm the applicability of an early theoretical picture [1] in manganites and further emphasize that phase coexistence can occur in any system in the presence of quenched disorder whenever two states are in competition through a FOPT. Here we show clear visual evidence of magnetic phase coexistence on micrometer scales in Ru-doped $CeFe_2$ alloys as the system is driven across a first order antiferromagnetic (AFM) to ferromagnetic (FM) transition. We explore how this phase coexistence evolves as a function of temperature, magnetic field, and time highlighting the generic features of a first order FM-AFM transition. The temporal evolution of the phase coexistence demonstrates that nucleation and growth can lead to percolation of a particular phase, and this observation has important implications for other systems [8,9] where percolative properties dominate macroscopic behavior.

$CeFe_2$ is a cubic Laves phase ferromagnet (with Curie temperature $\approx$230 K [10]), where a small substitution ($<$10%) of Co, Al, Ru, Ir, Os, and Re can induce a low temperature AFM state [11]. A giant magnetoresistance effect [12] and various memory effects [13,14] associated with the AFM-FM transition are well documented. We have chosen two $CeFe_2$ alloys with 4% and 5% Ru doping for our present work. The preparation and characterization of these polycrystalline alloys are described in Refs. [11,15]; the average grain size in standard samples as used here is usually more than 100 μm, and with a special annealing procedure grain size up to 5 mm has been reported [16]. Samples from the same batch have been well characterized [11–15,17]. Neutron diffraction studies of the same samples revealed a discontinuous change of the unit cell volume at the FM-AFM transition, confirming that it is first order [15]. Bulk magnetic measurements were made with a vibrating sample magnetometer (Oxford Instruments) and a SQUID magnetometer (Quantum Design-MPMS5). The magnetic field profiles close to the sample surface were obtained using a scanning Hall-probe system [18] with 5 μm square InSb Hall sensors. The sensor was scanned at a distance of 7 μm from the sample surface, each image comprising of 256 $\times$ 256 pixels. Fields up to 40 kOe can be applied, and the stray induction from the sensor is so small ($\approx$0.01 Oe) that it does not perturb the sample. Samples of various lengths (varying between 1 and 4 mm) and a 1.2 mm square cross section have been used to rule out any dominant role of demagnetization factor in the major findings of the present work.

Figure 1 shows the global magnetization (M) versus temperature (T) in an applied field (H) of 5 kOe for the $Ce(Fe_{0.95}Ru_{0.05})_2$ sample (Ru-5) obtained in the zero-field-cooled (ZFC) and the field-cooled cooling (FCC) mode. The paramagnetic (PM)-FM transition is marked by the rapid rise of M with decreasing T below 200 K, and it is thermally reversible. The FM-AFM transition is marked by the sharp drop in M below 90 K and shows substantial thermal hysteresis, which is an essential signature of a FOPT. We have obtained similar M-T curves for this sample as well as for the $Ce(Fe_{0.96}Ru_{0.04})_2$ sample (Ru-4) in various H. Thermal hysteresis is always present in the AFM-FM transition and broadens with increasing H, so that when $H > 30$ kOe (15 kOe) for Ru-5 (Ru-4) the $M_{FCC}(T)$ and $M_{ZFC}(T)$ curves fail to merge at least down to 20 K. The inset of Fig. 1 shows the schematic H-T phase diagram for the Ru-5 sample based on our $M(T)$

 0031-9007/04/92(14)/147203(4)$22.50

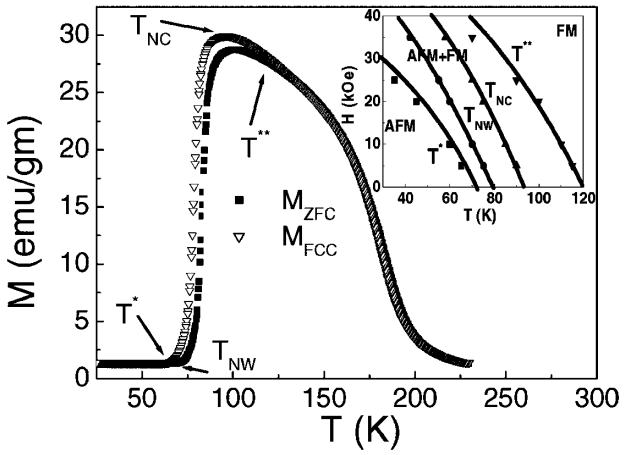

FIG. 1. M versus T in an applied H of 5 kOe for the Ru-5 sample, in the ZFC and FCC modes. The inset shows the H-T phase diagram representing T_{NW}, T_{NC}, T^*, and T^{**} (see text for their definitions) as a function of H. The value of T^* goes below 20 K when $H > 30$ kOe.

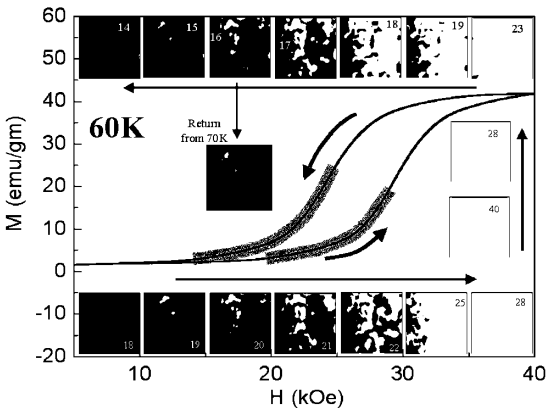

FIG. 2. Isothermal M versus the H plot and representative Hall-probe images at 60 K after cooling in zero magnetic field. Starting counterclockwise from the bottom left-hand corner, the images represent the AFM state in the ascending field cycle ($H = 18$ kOe), the AFM-FM transition regime in the ascending field cycle ($H = 19, 20, 21, 22, 25, 28$ kOe), the FM state ($H = 40$ kOe), the FM-AFM transition regime in the descending field cycle ($H = 28, 23, 19, 18, 17, 16, 15$ kOe), and the final AFM state ($H = 14$ kOe) at the end of the cycle. The frame below 16 kOe in the top row shows the effect of temperature cycling of 10 K on the supercooled FM state at 16 kOe. The shading scheme for the images is given in the text.

measurements with T_{NW} (T_{NC}) as the temperature of the sharp rise (fall) in M in the ZFC (FCC) path (see Fig. 1) which marks the onset of the AFM-FM (FM-AFM) transition while warming (cooling). T^* is the low T point where $M_{\mathrm{ZFC}}(T)$ and $M_{\mathrm{FCC}}(T)$ merges and T^{**} is the high T counterpart. A qualitatively similar phase diagram is obtained for the Ru-4 sample with lower characteristic temperatures. Note that $T_{NW}(H) < T_{NC}(H)$; i.e., the onset of nucleation of the AFM phase on cooling occurs at a higher T than does nucleation of the FM phase during warming. This is an indication of a disorder-influenced FOPT. As discussed below, the sector of the (H, T) phase diagram shown in the inset to Fig. 1 bounded by the $T_{NC}(H)$ [$T_{NW}(H)$] and $T^*(H)$ [$T^{**}(H)$] lines is metastable in nature and susceptible to energy fluctuations. We identify $T^*(H)$ [$T^{**}(H)$] with the low T (high T) limit of metastability in the free energy curves across a FOPT [19]. When the system is trapped in the metastable higher energy state it can be moved into the stable lower energy state by creating energy fluctuations such as by cycling T or H.

We now focus on phase coexistence and metastability across the FM-AFM transition region in isothermal field variation. In such isothermal experiments energy fluctuations (coming from k_BT term) remain constant all along the transition region. In Fig. 2 we present the isothermal M-H curve of the Ru-5 sample and Hall-probe images taken at representative fields around this M-H curve at 60 K. The sample used here is of dimension 2 mm $\times$ 1.2 mm $\times$ 1.2 mm, and the image frames are obtained by zooming on an area of 1 mm $\times$ 1 mm in the central portion of the sample. The field intensity distribution in these image frames is uniform in the FM and AFM states. Taking the field intensity of the FM state (which is much higher than that in the AFM state) as a reference, the AFM state is represented by intensity less than 20% of this value (black regions) while white regions represent intensities greater than 20%. We choose this 20% criterion to highlight the AFM-FM transition region marked by the dark band in the M-H curve in Fig. 2. In the ascending H cycle there is a sharp rise in M around 19 kOe indicating the onset of AFM-FM transition. In the H regime below 19 kOe the sample is entirely in the AFM state, and the corresponding image frames remain black. Around 19 kOe random white patches of high intensity local field appear in the image frames, indicating the onset of the FM phase in some parts of the sample. FM clusters of various size in the range of 5–20 μm are clearly distinguishable. The clusters grow in size and new clusters appear with a further increase in H, and some of those merge to give rise to even larger clusters in the range 20–100 μm; this process continues until the whole sample reaches the FM state [20]. While decreasing field from 40 kOe, along with bulk M the Hall images also show distinct thermal hysteresis. Traces of FM clusters remain down to 15 kOe, while the sample was completely in the AFM state in the regime $H < 19$ kOe in the ascending H cycle. We attribute this to supercooling of the FM state across the FOPT. We show here that a supercooled state, i.e., at 16 kOe in the descending H cycle, is susceptible to energy fluctuations. A small thermal perturbation in the form of an increase in temperature by 10 K and then bringing the sample back to 60 K again markedly decreases the amount of the supercooled-FM state. This is depicted in the image frame below the one of

16 kOe in the top row of images in Fig. 2. Note that the increase in T by 10 K should drive the system towards the higher temperature FM phase. However, the energy fluctuation associated with this temperature cycling is detrimental for the supercooled-FM state. We have seen the very same features of phase coexistence and metastability in Hall-probe images, on temperature variation across the AFM-FM transition while keeping the H constant. The detail results are not shown here for the sake of conciseness. We might expect to see a signature of superheating in the same way. The trace of the superheated AFM state would remain as a shaded region in an almost completely illuminated image frame. Better resolution of the images is required to reach a firm conclusion in this regard and locate an upper limit of metastability temperature (field) T^{**} (H^{**}).

The Hall-probe images taken across the FM-PM transition show a continuous decrease of uniformly distributed field intensity, which is consistent with a second order phase transition and confirms that the samples are macroscopically chemically homogeneous. We can further rule out gross chemical phase separation with the results of x-ray diffraction [11] and neutron scattering [15] studies. We assert here that purely statistical quenched compositional disorder, which is thought to give rise to "tweed structure" in the vicinity of martensitic transitions [3] and to phase separation in manganites[5–7], is at the root of the phase coexistence observed here. The influence of such intrinsic compositional disorder (through Ru substitutions) on the critical fluctuations phenomena at the second order PM-FM transition in the present $CeFe_2$ alloys has earlier been studied through detailed magnetic measurements [17].

The regions in the Ru-5 sample that go to the FM state first in the ascending H cycle (Fig. 2) are very different from those that transform first to the AFM state in the descending H cycle (Fig. 2). This is indicative of the local variation of the AFM-FM transition temperature T_N or field H_M leading to a rough $T_N(x, y)$ or $H_M(x, y)$ landscape. This distribution of T_N and H_M gives rise to the impression of global rounding of the transition in the bulk measurements. Our observation is in consonance with the disordered influenced FOPT proposed by Imry and Wortis [1]. A very similar disorder induced rough landscape picture has earlier been proposed for the vortex solid melting in the HTS material $Bi_2Sr_2CaCu_2O_8$ (BSCCO) [4] and materials with a premartensitic transition [3]. We have already seen that the traces of the supercooled-FM phase remain in fields well below the onset field of the FM state in the ascending H cycle. If there was a single FOPT field H_M (temperature T_N) the FM clusters would have appeared in the ascending H cycle in the sample first at the positions with relatively low energy barrier for the nucleation of the stable FM phase. Using the same argument, in the descending H cycle the stable AFM phase would appear first at these very points, and these spots should have been the spots of lower field intensity. However, the first FM patches not only survived in the descending H cycle, but some actually continued to exist as supercooled metastable FM states (see Fig. 2). The very same features are observed in the temperature variation measurements (not shown here). This again emphasized a rough $T_N(x, y)$-$H_M(x, y)$ landscape picture.

Figure 3 shows snapshots of the temporal evolution of the FM-phase clusters while undergoing the field induced AFM-FM transition. In these images T is fixed at 60 K and H is fixed at 20 kOe after starting from zero field in the ZFC condition. Twenty scanning Hall-probe images are taken over a period of 168 min and two representative images have been selected. Significant temporal growth of the FM clusters after their initial nucleation at random positions of the sample is clearly visible. This provides additional evidence of metastability in the phase-coexistence regime. This is also a strong indication that the AFM state is superheated at least in some regions of the sample.

We have observed qualitatively similar features of phase coexistence and metastability in the Ru-4 sample both in the bulk magnetization and Hall-imaging studies. In this sample with less doping the growth of the FM phase at the onset of the AFM-FM transition, both as a function of T and H, is faster than the Ru-5 sample. This relatively fast growth process along with the smaller number of nucleating clusters prohibited a clear-cut observation of the cluster size distributions in the phase-coexistence regime in the imaging experiments. This suggests that different disorder landscapes can control nucleation and growth with the key point that if the growth is slow enough, percolation will occur over an observable H (or T) interval before phase coexistence collapses. In the present study this is clearly true for the $x = 0.5$ sample. Percolative behaviors can be controlled by quite subtle changes in sample doping. The ramification to the manganite system, for example, is obvious.

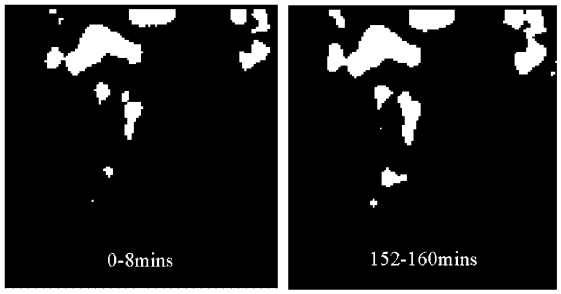

FIG. 3. Images showing temporal evolution of the phase coexistence at 20 kOe during the isothermal field induced AFM-FM transition at 60 K. Two images were taken 160 min apart, with each image taking 8 min of experimental time to complete. The sample area scanned and the shading scheme remain the same as in Fig. 2.

In conclusion, then, we have imaged the FM-AFM phase coexistence across the AFM-FM transition in Ru-doped $CeFe_2$ alloys. This AFM-FM transition bears distinct signatures of a FOPT, namely, supercooling, superheating, and time relaxation. We have imaged the temporal growth of the clusters inside the phase-coexistence regime for the first time and shown that this regime is quite sensitive to any energy fluctuations. Phase coexistence and metastability arise as a consequence of the intrinsic disorder-influenced FOPT [5–7]. The clusters in the present phase-coexistence regime have a size distribution in the range of 5–100 μm. This is larger than the length scale of 0.5 μm observed previously in manganites [5,8] and discussed in the existing theories [5–7]. The smallest size of clusters which can be detected in our present study is limited by the resolution of the Hall probe (5 μm). However, the growth and merger of the clusters as functions of T, H, and time lead naturally to the observation of a range of cluster size. It will be interesting now to see whether such a wide scale of cluster size distribution extending to micrometer scales is possible within the existing class of theoretical models [6,7] or whether our observation stimulates further theoretical refinement. Comparing further with the rough landscape picture of the vortex-matter melting transition [4], our observation highlights the generality of the phase-coexistence phenomenon. This in turn points to the possibility of the key role of intrinsic disorder-influenced FOPT in other classes of material of current interest, namely, giant magnetocaloric materials [21,22] and magnetic shape memory alloys [23].

S. B. R. acknowledges financial support from EPSRC, UK.

[1] Y. Imry and M. Wortis, Phys. Rev. B **19**, 3580 (1979).
[2] H. Scjhremmer, W. Kleemann, and D. Rytz, Phys. Rev. Lett. **62**, 1896 (1989).
[3] S. Kartha, J. A. Krumhansl, J. P. Sethna, and L. K. Wickham, Phys. Rev. B **52**, 803 (1995).
[4] A Soibel *et al.*, Nature (London) **406**, 282 (2000).
[5] E. Dagotto, T. Hotta, and A. Moreo, Phys. Rep. **344**, 1 (2001); E. Dagatto, *The Physics of Manganites and Related Compounds* (Springer, New York, 2003), and references therein.
[6] A. Moreo *et al.*, Phys. Rev. Lett. **84**, 5568 (2000).
[7] J. Burgy *et al.*, Phys. Rev. Lett. **87**, 277202 (2001).
[8] M. Uehara, S. Mori, C. H. Chen, and S. W. Cheong, Nature (London) **399**, 560 (1999).
[9] L. Zhang *et al.*, Science **298**, 805 (2002).
[10] L. Paolisini *et al.*, Phys. Rev. B **58**, 12 117 (1998), and references therein.
[11] S. B. Roy and B. R. Coles, J. Phys. Condens. Matter **1**, 419 (1989); Phys. Rev. B **39**, 9360 (1990).
[12] H. Kunkel *et al.*, Phys. Rev. B **53**, 15 099 (1996).
[13] M. A. Manekar *et al.*, Phys. Rev. B **64**, 104416 (2001).
[14] M. K. Chattopadhyay *et al.*, Phys. Rev. B **68**, 174404 (2003); K. J. S. Sokhey *et al.*, Solid State Commun. **129**, 19 (2004).
[15] S. J. Kennedy and B. R. Coles, J. Phys. Condens. Matter **2**, 1213 (1990).
[16] S. J. Kennedy, P. J. Brown, and B. R. Coles, J. Phys. Condens. Matter **5**, 5169 (1993).
[17] D. Wang, H. P. Kunkel, and G. Williams, Phys. Rev. B **51**, 2872 (1995).
[18] G. K. Perkins *et al.*, Supercond. Sci. Technol. **15**, 1156 (2002).
[19] P. M. Chaikin and T. C. Lubensky, *Principles of Condensed Matter Physics* (Cambridge University Press, Cambridge, England, 1995); P. Chaddah and S. B. Roy, Phys. Rev. B **60**, 11 926 (1999).
[20] This 20% criterion may give the wrong impression that the formation of the FM state is completed by 26 kOe. The FM state actually goes on developing in the ascending H path until 35 kOe, and these developments can be seen with a higher ($> 20\%$) threshold criterion. See EPAPS Document No. E-PRLTAO-92-012414 for a movie of the AFM-FM transition process in ascending and descending H cycles. A direct link to this document may be found in the online article's HTML reference section. The document may also be reached via the EPAPS homepage (http://www.aip.org/pubservs/epaps.html) or from ftp.aip.org in the directory /epaps/. See the EPAPS homepage for more information.
[21] B. Teng *et al.*, J. Phys. Condens. Matter **14**, 6501 (2002).
[22] V. Pecharsky *et al.*, Phys. Rev. Lett. **91**, 197204 (2003).
[23] W.-H. Wang *et al.*, Phys. Rev. B **65**, 012416 (2001).